CBM-PHYS-note-2005-001
I3HP-FutureDAQ-note-2005-002
23 June 2005

Analysis of D^0 meson detection in Au+Au collisions at 25 AGeV

Sergey Gorbunov[1], Ivan Kisel[2] and Iouri Vassiliev[3]

[1]Deutsches Elektronen-Synchrotron DESY, Zeuthen, Germany
[2]Kirchhoff-Institut für Physik, University of Heidelberg, Germany
[3]Gesellschaft für Schwerionenforschung mbH, Darmstadt, Germany

Abstract

The note studies feasibility of the D^0 mesons exclusive reconstruction in the hadronic decay channel ($K^- + \pi^+$). It will provide a direct measurement of charm kinematic distributions, one of the major experimental challenges of the CBM experiment. The key role of the successful D^0 detection strategy are tracks finding and fitting in the inhomogeneous magnetic field, primary and detached D^0 vertex reconstruction, many orders of magnitude background suppression keeping D^0 detection efficiency as high as possible. High resolution secondary vertex determination realized by using MAPS detectors. Estimated correspondent D^0 detection rate is about 1000 per day with an interaction rate of 0.1 MHz and signal to background ratio is approximately 3.

1 Introduction

One of the main goals of the CBM experiment [1] is to study the behavior of nuclear matter in the conditions of high densities and temperatures in which the transition to a deconfined quark gluon plasma phase [2] is expected. One of the signatures of this new state is enhanced production of strange [3] and charm [4] particles. In addition, the ratio between antiparticle and particle yields measured at mid-rapidity have attracted special interests in studies of the dependence of AA collision dynamics upon collision energy [5].

Open charm measurement is one of the primary interest of the CBM experiment, and the one of the most difficult tasks as well.

The difficulties of this measurement are very low multiplicity of D mesons production $(1.2 - 1.8) \times 10^{-4}$ per central Au+Au event at 25 AGeV (as predicted by the HSD model [6]) within an environment of 900 charged hadrons produced in a collision and relatively low branching ratio of D^0 decays into the $K^- + \pi^+$ channel (3.8%). Most of the charged hadrons are emitted from the primary vertex and can be identified and suppressed by many orders of magnitude by an impact parameter cut for each of the two decay product tracks and an additional cut on the z-position of the secondary vertex cut, but hyperon decays close to the primary vertex require special treatment.

The expected observable effects are: interaction of the produced charm quarks with the plasma may reduce their momenta because of elastic collisions and in-medium gluon emissions [7]; secondary parton scattering in the produced high-density partonic system may provide an additional source of charm quarks [4]. The exclusive reconstruction of D^0 mesons in the hadronic decay channel ($K^- + \pi^+$) will provide a direct measurement of the charm kinematic distributions.

The D^0 detection strategy discussed in the note takes into account the specific STS geometry and is based on precise reconstruction of the event topology.

2 Signal and background simulation

To study feasibility of the D^0 measurement in the CBM experiment 10^5 background Au+Au central UrQMD events at 25 AGeV have been simulated. A signal pair ($K^-\pi^+$) from D^0 decay has been added to each event in order to simulate the signal in the environment of background hadrons. Fig. 1 shows the initial distribution of transverse momentum p_t versus rapidity Y (left plot) and the distribution of z-vertices for the simulated signal $D^0 \rightarrow K^- + \pi^+$ (right plot). The z coordinate axis corresponds to the beam direction.

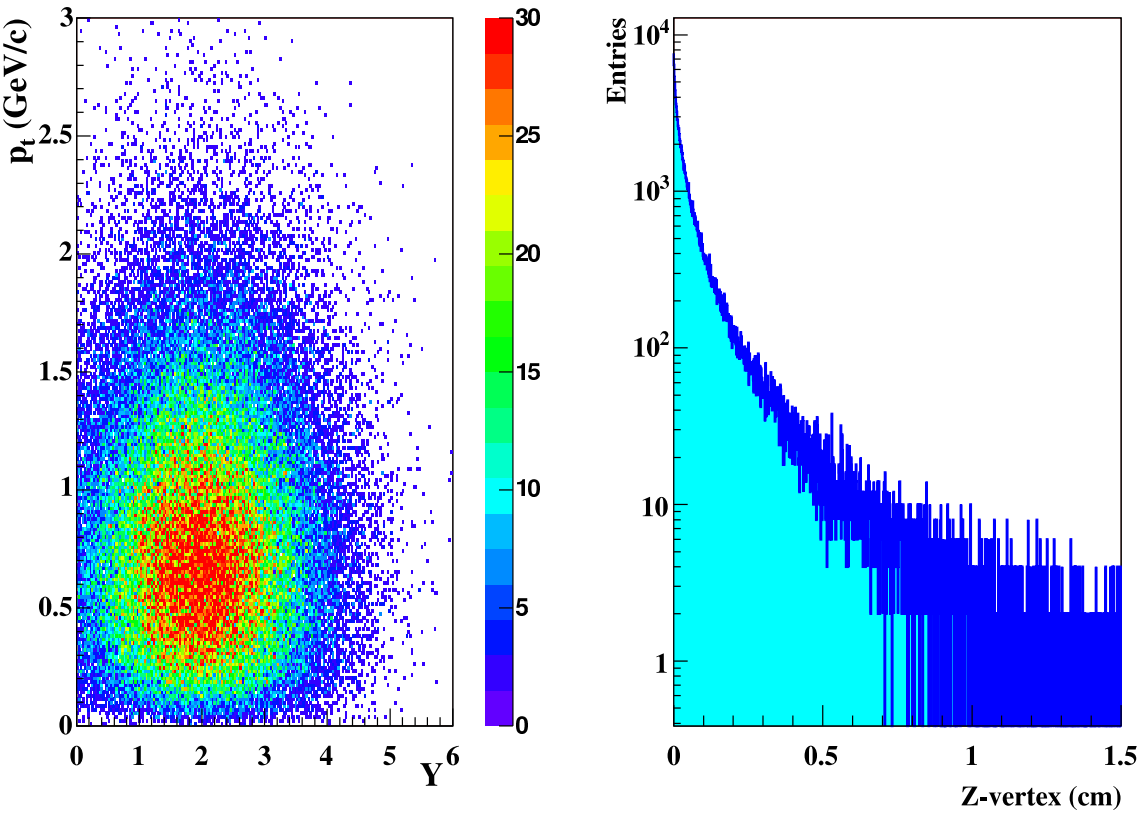

Figure 1: Initial distribution of transverse momentum p_t versus rapidity Y (left plot) and distribution of z-vertices (right plot) for MC generated events $D^0 \rightarrow K^- + \pi^+$

Background and signal plus background events have been processed using the GEANT3 based detector simulation tool CBMROOT.

In the simulations we used the STS detector of 7 stations positioned at 5, 10, 20, 40, 60, 80 and 100 cm from the target made of 250 μm thick gold plate. The first 3 stations are placed in vacuum in order to decrease effect of multiple scattering in the carbon beam tube on track parameters at the target. Each station has thickness of 200 μm. Monte Carlo (MC) track impact

points have been smeared with the Gaussian function assuming typical values of $\sigma = 3$ μm for the first two Monolithic Active Pixel Sensors (MAPS) stations close to the target and $\sigma = 10$ μm for the other five silicon strip stations downstream. All detectors have idealized response (no fake hits, efficiency losses, pile-up etc.). The asymmetric magnetic field has been used to trace particles through the detector.

3 Event reconstruction

Event reconstruction has been done using the cellular automaton and Kalman filter based procedures [1]. Propagation of tracks in the asymmetric inhomogeneous magnetic field is based on the analytic formula [8].

For evaluation purposes of the track finding procedure all simulated and reconstructed tracks are subdivided into several categories. The all set comprises tracks which intersect the sensitive regions of at least four tracking stations. A reference track should in addition have a momentum greater than 1 GeV/c. The reference set of tracks can also include tracks of particular physics interest such as secondary tracks from interesting decays and primary tracks coming from the target region. In addition to these tracks, the extra set of tracks, containing low-momentum tracks, is also considered.

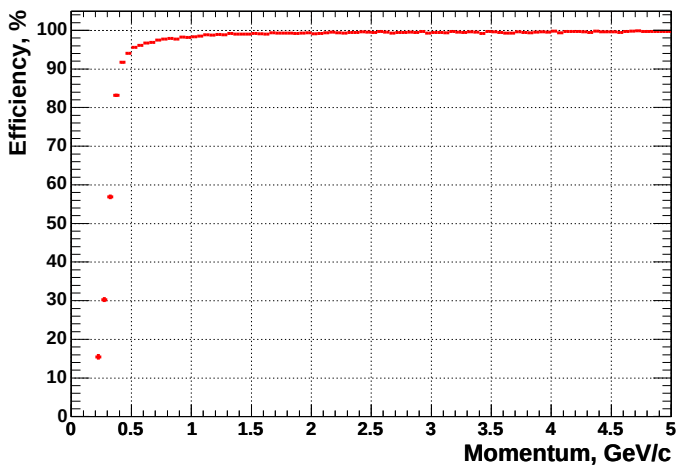

Figure 2: Track reconstruction efficiency versus momentum of particle in the STS detector

A reconstructed track is assigned to a generated particle if at least 70% of its hits have been caused by this particle. A generated particle is regarded as found if it has been assigned to at least one reconstructed track. If the particle is found more than once, all additionally reconstructed tracks are regarded as clones. A reconstructed track is called ghost, if it is not assigned to any generated particle (using 70% criteria).

The total reconstruction efficiency (see Fig. 2) for all tracks is about 97%. The reconstruction efficiency clearly depends on the particle momentum. High energetic particles (here they form the reference set of tracks, see Table 1) have efficiency larger than 99%. Secondary tracks from D^0 decay have momentum larger than 1 GeV/c and, in addition, come from the target region, which can be used during the reconstruction, and, therefore, they have even higher efficiency of 99.90%. Let us note that only simple Gaussian smearing was used, and no double hit effects in the sensor considered. Most of other secondary tracks are low energetic tracks and suffer significant multiple scattering in the detector material. The efficiency of low energetic tracks (the extra set of tracks) is about 90%. Particles with momentum lower than 200 MeV/c are

mostly out of geometrical acceptance of the STS detector. There is no splitting of reconstructed tracks into short parts as it can bee seen from the clone rate, which is negligible. The level of wrong reconstructed tracks (ghost tracks) is less than 1% and these tracks are similar to tracks of short low energetic particles.

Track category	Efficiency (%)
D0	99.90
Refset	99.40
Allset	96.93
Extra	89.50
Clone	0.01
Ghost	0.80
Tracks/event	554

Table 1: Efficiencies of the track reconstruction in the STS detector for different sub-sets of tracks

Parameter	Resolution	Pull
x	27 μm	1.04
y	26 μm	1.00
t_x	1.5 mrad	1.04
t_y	1.5 mrad	1.03
p	0.69 %	1.19
p_{π^+}	0.67 %	1.20
p_{K^-}	0.67 %	1.20
p_{pv}	0.63 %	1.21

Table 2: Resolutions and pulls of fitted track parameter distributions at the track vertex z-position. Momentum resolution is given without (p) and (for primary tracks only) with (p_{pv}) constraint to the primary vertex

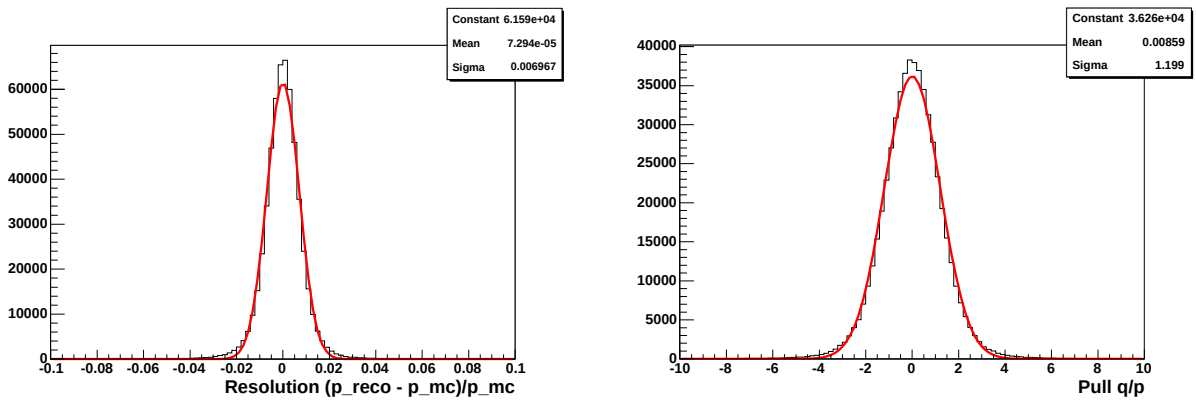

Figure 3: Residuals and normalized residuals of the estimated track momentum at the track vertex z-position obtained from 1000 events of central Au+Au collisions at 25 AGeV in the asymmetric inhomogeneous magnetic field

Table 2 and figure 3 show residuals and normalized residuals (pulls) of the track parameters at the track vertex z-position. Pion particle mass hypothesis is used at this stage to fit tracks.

A measure of the reliability of the fit are the pull distributions of the fitted track parameters. The reconstructed track parameters and covariance matrix at the vertex where the track originates are obtained by propagating the track parameters at the measurement position closest to the vertex, taking into account the remaining material traversed.

Table 2 shows the RMS of the Gaussian fits to the residual and normalized residual distributions. All pulls are centered at zero indicating that there is no systematic shift in the reconstructed track parameter values. The distributions are well fitted using Gaussian functions with small tails caused by the various non-Gaussian contributions to the fit. The q/p pull shows slightly underestimated errors. This can be a result of several approximations made in the fitting procedure mainly in the part of material treatment.

Mean relative momentum resolution for all tracks is 0.69%. Secondary tracks from D^0 decay being longer have slightly better momentum resolution of 0.67%. After the primary vertex is reconstructed, tracks identified as primary can be refitted with an additional constraint to the primary vertex position. This improves considerably their average track momentum resolution to 0.63%.

Parameter	Resolution (μm)	Pull
x_v	0.71	1.06
y_v	0.61	1.04
z_v	3.99	1.02

Table 3: Residuals and normalised residuals (pulls) of the primary vertex parameters obtained on 1000 events of central Au+Au collisions at 25 AGeV in the asymmetric inhomogeneous magnetic field

The primary vertex was determined from all tracks reconstructed in the STS excluding those which formed well detached vertices like K_S^0 and Λ decays. The Kalman filter based algorithm reconstructs the primary vertex with high accuracy (see Table 3).

The method of geometrical fitting of secondary vertex is also based on the Kalman filter. The algorithm proceeds track by track and finally obtains the estimates of the vertex position and smoothed parameters estimates of the tracks composing the vertex together with the corresponding covariance matrix.

Parameter	G	G+M	G+T	G+M+T
x_v	7.6	7.6	1.8	1.7
y_v	7.1	7.0	1.9	1.7
z_v	47.7	46.1	46.0	44.4
p_{π^+}	0.65	0.49	0.62	0.45
p_{K^-}	0.66	0.54	0.62	0.50

Table 4: Accuracy (in μm) of the secondary vertex parameters and relative momentum resolution $\delta p/p$ (in %) of the secondary tracks obtained from 10^5 D^0 decays in the inhomogeneous magnetic field by applying different sequences of the vertex fitting routines: the geometrical (G) fit and the fits with mass (M) and topological (T) constraints

Table 4 shows the residuals and the normalized residuals of the D^0 decay vertex parameters. Pulls show that the errors are well estimated. The longitudinal resolution is 48 μm. Particle hypotheses have been used in the track fit procedure to properly account for multiple scattering effects.

Precision of the secondary vertex parameters obtained in the geometrical vertex fit can be improved by taking into account several assumptions on tracks associated to the vertex. Two types of constraints have been included into the secondary vertex fit: a mass constraint and a topological constraint. The mass constraint is usually applied in the case of one or several combinations of particles in the vertex are known to originate from a narrow width mass state. The topological constraint is used to point a mother particle to the (already reconstructed) primary vertex.

Fig. 4 and table 4 show residuals and normalized residuals of the D^0 decay vertex parameters obtained by the full chain of the vertex fitting algorithms. The pull of the secondary vertex

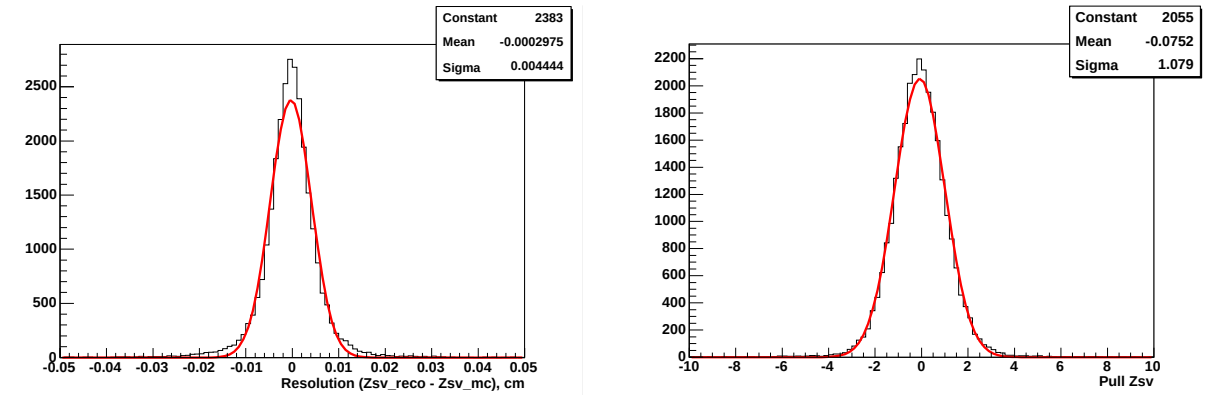

Figure 4: Residuals and normalized residuals (pulls) of the secondary vertex z-position obtained from 10^5 D^0 decays in the inhomogeneous magnetic field by applying the full sequence of the vertex fitting routines: the geometrical fit and the fits with mass and topological constraints

z-position shows that the vertex parameters are well estimated. The longitudinal resolution is improved comparing to the geometrical fit and now equals 44 μm. Particle hypotheses have been used during the track fits to properly account for multiple scattering effects, and in the vertex fit procedure to apply the constraints.

Table 4 gives also the accuracy of the secondary vertex parameters for different combinations of the vertex routines. One can see that the mass constraint mainly improves the z-position of the vertex, while the topological constraint increases the resolution of the transversal parameters of the secondary vertex position. The best resolution is reached by applying both, mass and topological, constraints.

Table 4 shows also the relative momentum resolutions of the secondary tracks at different stages of the event reconstruction. The mass constraint secondary vertex fit gives the most significant improvement of the momentum resolution for both particles. The best accuracy is reached applying all constraints. The difference in the momentum resolution behavior of π^+ and K^- is probably due to their masses.

4 D^0 detection strategy

The prime goal of the D^0 detection strategy is a many orders of magnitude background suppression and, at the same time, achieving maximum of efficiency for the signal. For the background suppression several main cuts have been defined and applied in the following order:

1. χ^2 cut together with upper and lower values cuts on the track impact parameter;
2. track momentum p-cut;
3. track transverse momentum p_t-cut;
4. χ^2 cut on the two-tracks secondary vertex geometrical fit;
5. cut on z-position of the secondary vertex;
6. cut on D^0 reconstructed momentum pointing to the primary vertex;
7. χ^2 cut on D^0 distance to the primary vertex.

Optimization of the cuts has been achieved by maximizing the ratio $S/\sqrt{B}$ in the cases, where the background is dominated, or $S/\sqrt{S+B}$, where S is the number of accepted signal events in the Monte-Carlo $D^0 \rightarrow K^- + \pi^+$ sample and B is the number of background UrQMD events, observed in the whole invariant mass region. As an example, the left part of the Figure 5 shows the transverse momenta distribution for the background events as black line and for the signal K^- from the D^0 decay as red line. The right part of the Figure 5 gives the ratio $S/\sqrt{S+B}$ and the achieved threshold (vertical blue line) at $p_t = 0.5$ GeV/c, where the function $S/\sqrt{S+B}$ has maximum.

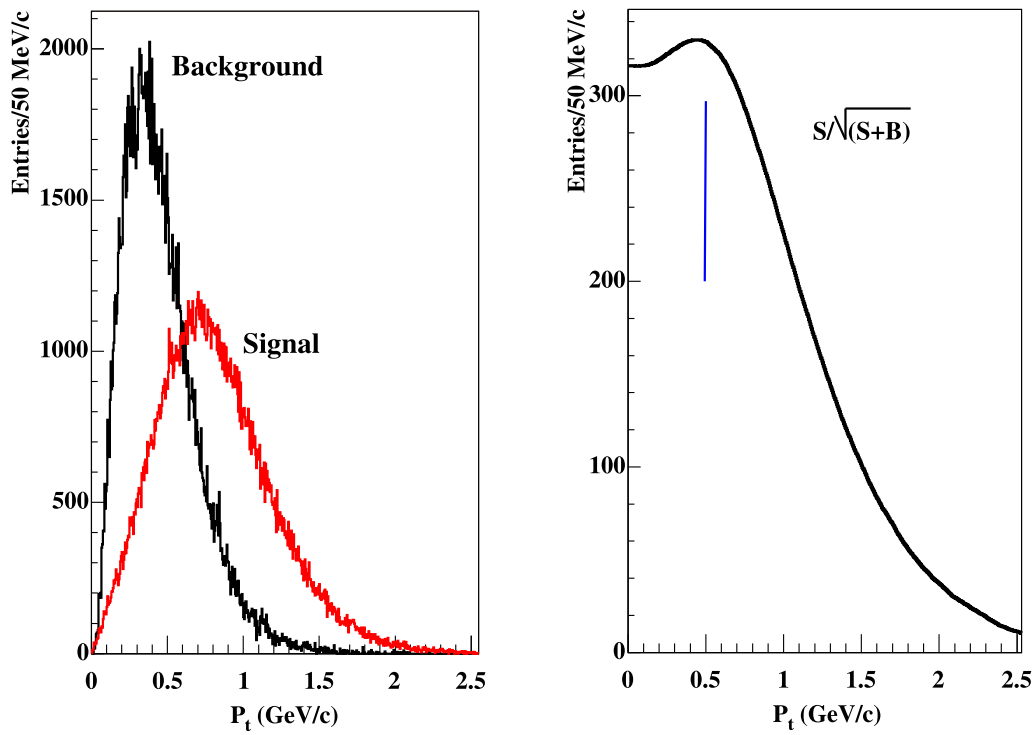

Figure 5: Left part: transverse momentum distribution for the emitted kaons K^- from the D^0 decay (red line) and the background (black line). Right part: the ratio $S/\sqrt{S+B}$ with maximum at $p_t = 0.5$ GeV/c.

The D^0 meson decays through a week process and a mean proper length $c\tau = (123.7 \pm\ 0.8)\ \mu$m. Consequently, in case of D^0 decaying into $K^- + \pi^+$ these two tracks have relatively big impact parameter and the distance between the primary vertex and decay point is measurable. Since the majority of the primary tracks have very small impact parameter, significant part of the combinatorial background can be rejected using the impact parameter cut. The left part of the Figure 6 shows the impact parameter distribution for the signal as red line and for the background as black line. The right part gives the ratio $S/\sqrt{B}$ with the maximum at 80 μm marked by the vertical blue line.

The achieved optimized impact parameter cut value of 80 μm decreases strongly ($\approx$ 4 times) the signal efficiency. Nevertheless, K^- and π^+ tracks from D^0 decay have an average momentum of about 5.5 GeV/c and their corresponding errors of the tracks propagated to the target plane are significantly smaller then the errors of background "soft" track pairs. Therefore, the χ^2 distance cut between the primary vertex and the track impact point to the target plane is more selective

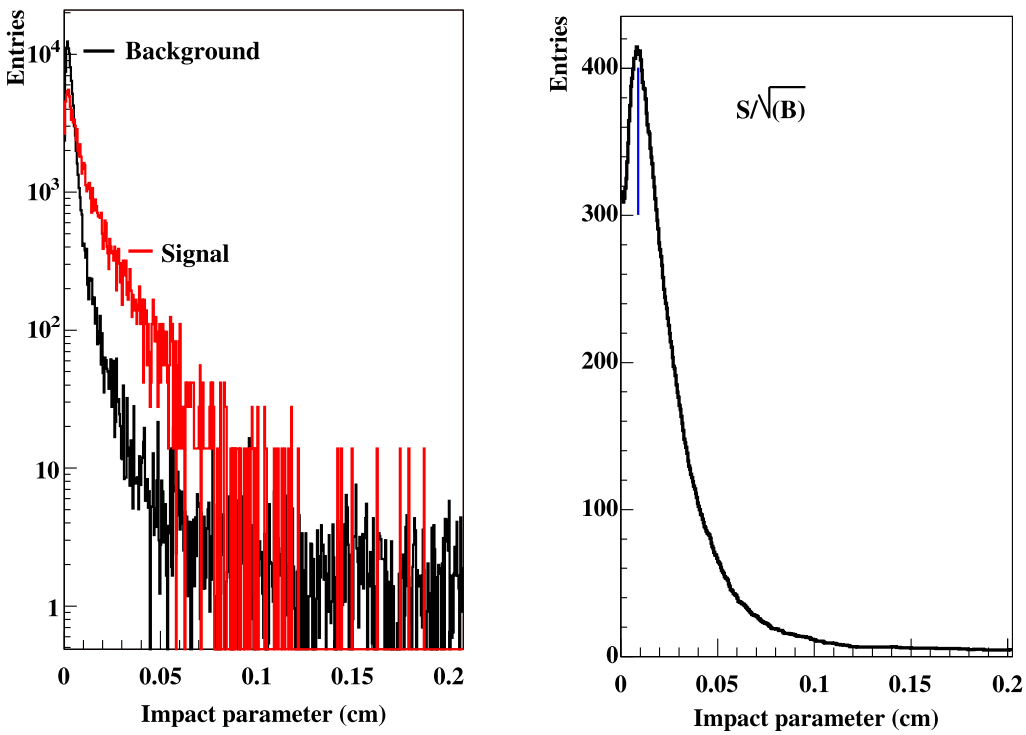

Figure 6: Left part: impact parameter distribution for the emitted kaons K^- and π^+ from the D^0 decay (red line) and the background (black line). Right part: the ratio $S/\sqrt{B}$ with the maximum at 80 μm.

and effective. The Figure 7 shows the impact parameter distribution for the selected $K^-\pi^+$ tracks from D^0 decay with $\chi^2 < 2.2\ \sigma$. This value has been calculated in order to keep the same background rejection factor (≈ 1000) as with an 80 μm impact parameter cut. It can be seen from the Figure 7, that found signal tracks in some cases have an impact parameter of as low as 40 μm. Thus, using the χ^2 cut allows to increase the signal efficiency up to 25% keeping the same background rejection factor.

Part of the primary tracks can also create detached secondary vertices due to multiple scattering in the STS detector. In order to take into account this combinatorial background, the distribution of the secondary vertices has been produced with UrQMD events. As it is shown on the Figure 8, the background secondary vertex spectra (black line) has the expected maximum at $z = z_{\text{target}}$. The upstream tail is the result of the multiple scattering in the target and in the STS stations (combinatorial background), while in the downstream tail the hyperons decay depending background is present in addition.

The reconstructed signal secondary vertices from the $D^0 \rightarrow K^- + \pi^+$ decays are shown with red line. The significant difference in shape of the signal and background spectra allows to optimize the z-vertex cut by maximizing the ratio $S/\sqrt{S+B}$ (significance) as it was done for the p_t-cut. The clear maximum of the significance function at 250 μm is shown in the right part of the Figure 8. All cuts have been optimized by the above described procedure and the obtained values are given in the Table 5.

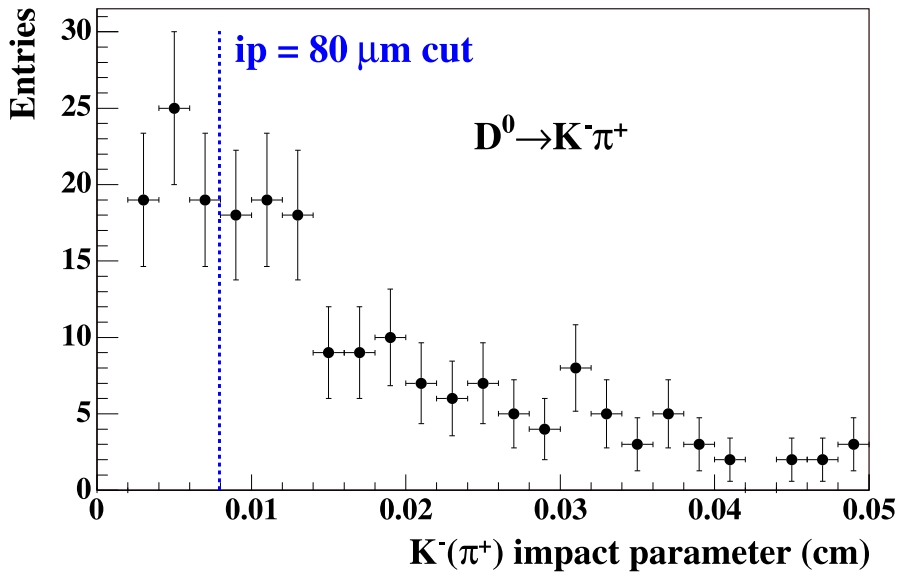

Figure 7: Impact parameter distribution for the selected $K^-\pi^+$ tracks from D^0 decay with $\chi^2 < 2.2\sigma$. First three bins are not taken into account in case of using the impact parameter 80 μm cut

Relatively small amount of material of the first two STS stations, high space point resolution (σ =3 μm) and large average K^- and π^+ momenta allow to achieve D^0 secondary vertex resolution of 39 μm.

On the Figure 9 is shown the difference between MC and reconstructed z-position of the vertices for $D^0 \rightarrow K^- + \pi^+$. Resolution of 39 μm allows to separate good enough detached secondary vertices from the primary vertex, due to the lifetime of the D^0 mesons being $c\tau = 123.7$ μm. In order to reconstruct properly a secondary vertex for the background track pairs, the geometrical secondary vertex fit procedure has been used. The topological constraint fit increases significantly signal events selection and describes properly the central part of the Gaussian distribution and the tails as well.

The main background contributions expected in the 3σ region of the invariant mass peak are due to combinatorics and hyperons decays, mainly K^0_S and Λ, $\Sigma^{+(-)}$, Ξ^- and Ω^-. A single UrQMD event contains on average 7.6 K^0_S and 10.5 Λs within the geometrical acceptance. The combinatorial background is suppressed mainly by the track impact parameter χ^2-cut, z-vertex cut, as well as by D^0 pointing cut (when one track from D^0 decay is combined with multiple scattered track), p_t-cut, vertex χ^2-cut and p-cut. The influence on the invariant mass spectra shape of "one-track" cuts is illustrated on the Figure 10, where 10^3 UrQMD events were mixed with $D^0 \rightarrow K^- + \pi^+$ events. The magenta line shows the MC invariant mass spectra with perfect particle identification, the light blue histogram represents the background and signal without particle identification after applying all single track cuts, the blue line — the background (and signal) with z-vertex greater then 250 μm and, finally, the red histogram is the reconstructed 104 signal events, corresponding to a 10.4% reconstruction efficiency.

The background due to hyperons decay is suppressed by the track impact parameter cut (upper value) and by removing from the final invariant mass spectra tracks from K^0_S and Λ decays. These particles were identified by Armenteros-Podolanski technique. On the Figure 11 is shown

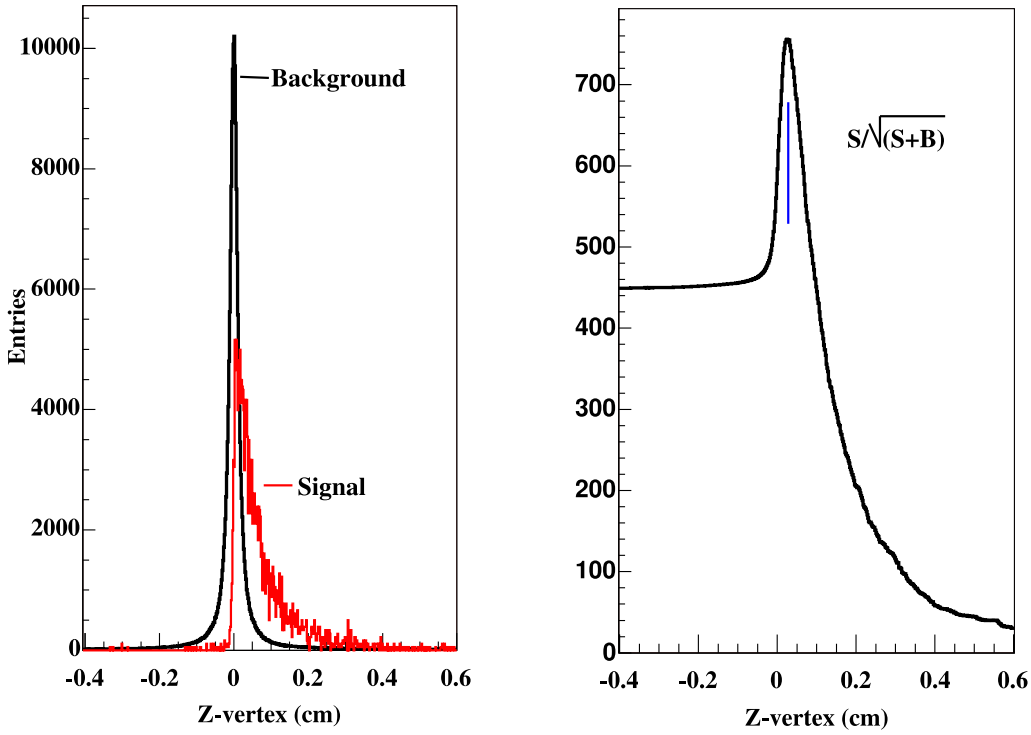

Figure 8: Left part: reconstructed secondary vertices for the background (black line) and for the signal (red line). Right part: the ratio $S/\sqrt{S+B}$ with maximum at $z = 250$ μm.

the transverse momentum $\tilde{p}_t$ of the opposite charged decay products versus their asymmetry in longitudinal momenta $p_L^{\pm}$. In each event a full combinatorial search for K_S^0 and Λ had been performed. The minimum distance between two opposite charged tracks that formed a vertex downstream the primary vertex was required to be less than 0.5 mm and correspondent vertex χ^2 value should be less than 5.0. Clusters of the events shaped according to the kinematics of $K_S^0 \to \pi^+\pi^-$ and $\Lambda \to p\pi^-$ decays are clearly visible. A cut $\tilde{p}_t \cdot c\tau > 0.23$ GeV/c·cm was applied to reduce the background from K_S^0 and Λ decays, where $\tilde{p}_t$ is the transverse momentum relative to the K_S^0 or Λ line-of-flight and τ is their proper lifetime.

Excluding K_S^0 and Λ decay products from the final invariant mass spectrum decreases the hyperons decay depending background by the factor of two.

5 Analysis and results

Amount of collected D^0s can be calculated as $N_{D^0} = BR \cdot M_{\rm mb} \cdot \epsilon \cdot N_{\rm mb}$, where BR is the branching ratio of D^0 decaying into the $K^- + \pi^+$ channel (3.8%), $M_{\rm mb}$ is the multiplicity of D mesons production 0.4×10^{-4} per minimum bias Au+Au event at 25 AGeV, ϵ is D^0 detection efficiency and $N_{\rm mb}$ is the number of minimum bias interactions. The obtained efficiency ϵ of 10.4% allows us to collect about $1.5 \cdot 10^5 D^0$ per 10^{12} minimum bias interactions keeping the rejection factor of 1000 for the minimum bias events. The amount of 10^{12} minimum bias events is the current limit for the MAPS detectors lifetime due to radiation hardness in the CBM experiment [1]. It corresponds to about 4 months of data taking at interaction rate of

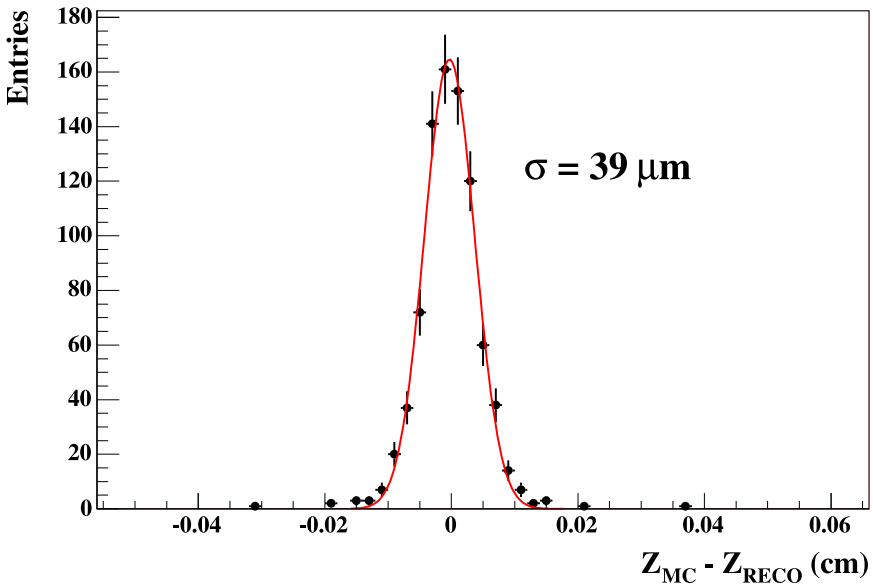

Figure 9: Z-vertex resolution after the geometrical and topological fit for the D^0 decaying into $K^- + \pi^+$.

10^{-1} MHz. The trigger rejection factor is a ratio of generated minimum bias events to trigger accepted ones, where accepted events are those, which produce an entry(s) in the invariant mass spectrum in the range 0.5–4.0 GeV. The shape of the background in the range 1.8–2.0 can be seen in the Figure 12.

A rejection factor of 1000 is sufficient for the first level event selection and allows to take 10^{12} interactions. In a physics analysis, a further background rejection by 10^6 is needed to achieve an adequate signal to background ratio. This can be done in different ways using information from non STS sub-detectors. The background origin study shows that 76% of background events were produced with proton tracks. Such type of backgrounds was eliminated by proton identification technique using TOF sub-detector [1]. In order to increase selectivity of secondary tracks the χ^2 distance cut between the primary vertex and the track impact to the target plane was also increased to 3.5 σ comparing with 2.2 σ at the rejection factor of 1000. As a results the efficiency of D^0 detection decreases from 10.4% to 8.5%. After all cuts applied we have derived the background suppression factor of 10^5 in the signal mass region.

cut	**optimized value**	**signal efficiency, %**
χ^2 distance to the primary vertex	3.5 (2.2) σ	53 (65)
p-cut	1.0 GeV/c	72
p_t-cut	0.5 GeV/c	61
z-vertex cut	250 μm	54
D^0 pointing cut	30 μm	99
geometrical vertex χ^2cut	$\leq$5	91
all cuts	–	8.5 (10.4)

Table 5: Optimized cut values

The optimized cut values together with the signal efficiency for the rejection factor of 10^5 in

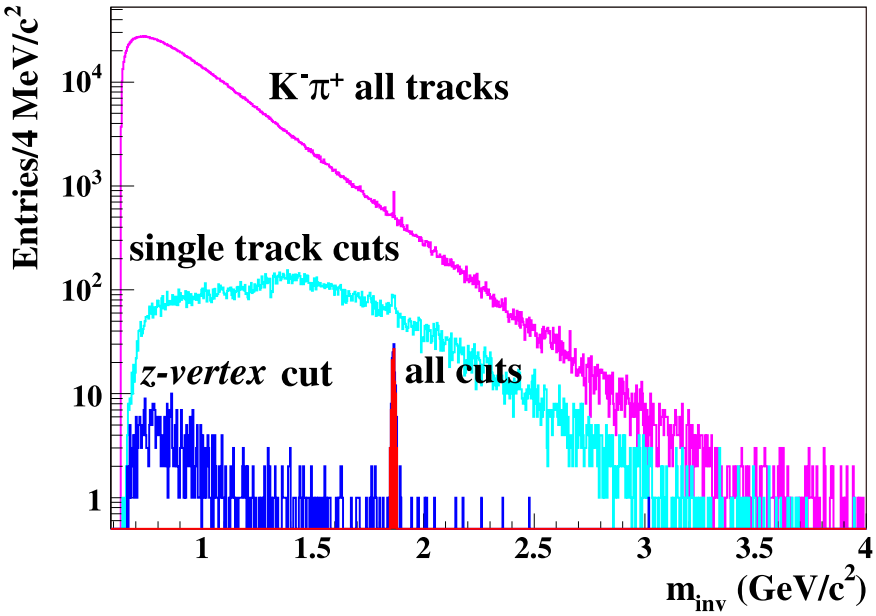

Figure 10: Monte Carlo and reconstructed invariant mass spectra after applying various cuts. Magenta line is perfect particle identification cut, light blue histogram — the background and signal without particle identification after applying all single track cuts, blue line — the background (and signal) with z-vertex greater then 250 μm cut and red histogram is the reconstructed signal (104 events)

the signal mass region are shown in the Table 5. The values for the trigger rejection factor of about 1000 are given in brackets.

Let us note that in order to calculate the signal to background ratio with so high background suppression factor at least few times 10^7 MC events needs to be simulated. This is a very time consuming task and in order to estimate the shape of the background in the signal invariant mass region the so-called "MC super-event" technique was used. A MC super-event was constructed from 10^3 UrQMD minimum bias events transported through the STS. Since the amount of background entries in the invariant mass spectra increases quadratically with the number of tracks, one super-event is equivalent to 10^6 UrQMD minimum bias events. Using obtained invariant mass background spectrum shape and the signal efficiency, the resulting background plus signal spectrum is shown in the Figure 12.

The spectrum is the result of 10^{12} minimum bias interactions and is equivalent to roughly 4 months of data taking at 0.1 MHz interaction rate. The corresponding D^0 detection rate is about 1000 per day.

6 Conclusions

The MC simulations of D^0 mesons hadron decay into the $K^- + \pi^+$ channel show feasibility of D^0s collection rate about 1000 per day using combination of 2 MAPS and 5 strip STS stations of the CBM detector. The developed track finding and track fitting in the inhomogeneous magnetic field procedures allow to obtain the 8 MeV invariant mass resolution. The resolution of D^0 vertex is about 39 μm in longitudinal direction. The efficiency of D^0 detection is 8.5%.

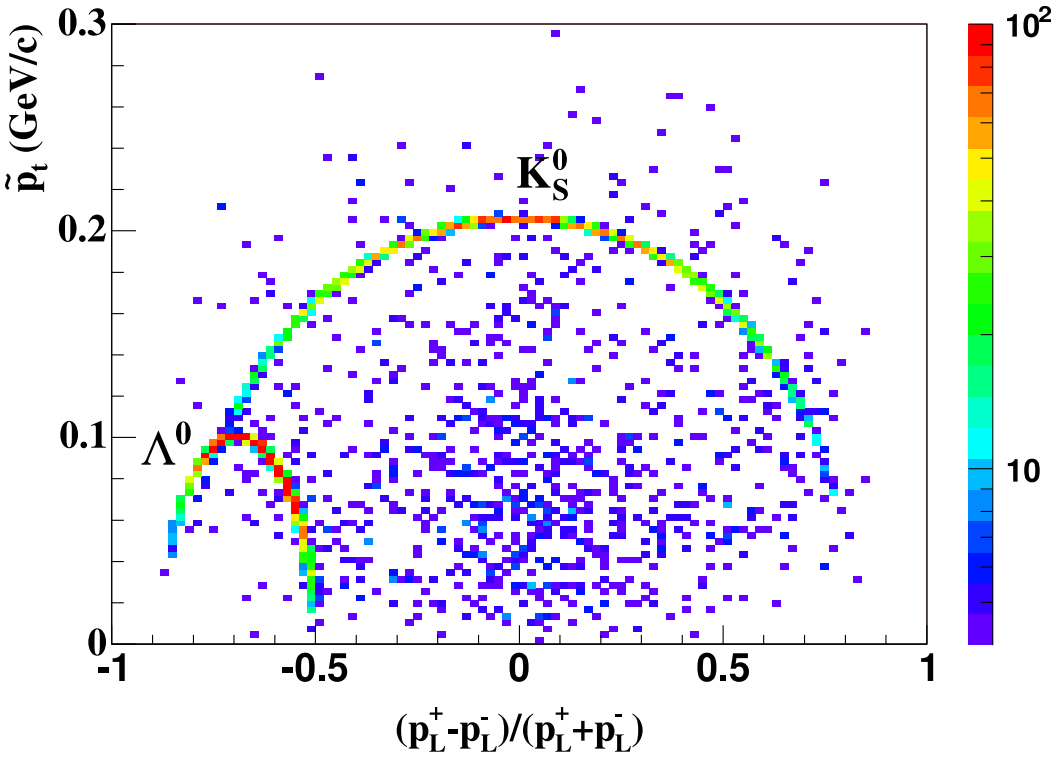

Figure 11: The Armenteros-Podolanski plot: transverse momentum $\tilde{p}_t$ of the oppositely charged decay products versus their asymmetry in longitudinale momenta $p_L^{\pm}$

The achieved signal to background ratio is about 3 in the $\pm$ 2σ invariant mass region. The maximal data taking rate can be 10 MHz, however in this case one hase to take into account pile-up in MAPS detectors.

7 Acknowledgements

We acknowledge the support of the European Community-Research Infrastructure Activity under the FP6 "Structuring the European Research Area" programme (HadronPhysics, contract number RII3-CT-2004-506078).

References

[1] CBM Experiment, Technical Status Report, January 2005, (`http://www.gsi.de/onTEAM/dokumente/public/DOC-2005-Feb-447_e.html`).

[2] Proc. 15th Int. Conf. on Ultra-Relativistic Nucleus-Nucleus Collisions (QM2001), Nucl. Phys. **A698** (2002) Issue 1–4.

[3] S.A. Bass et al., Last call for RHIC predictions, Nucl. Phys. **A661** (1999) 205c.

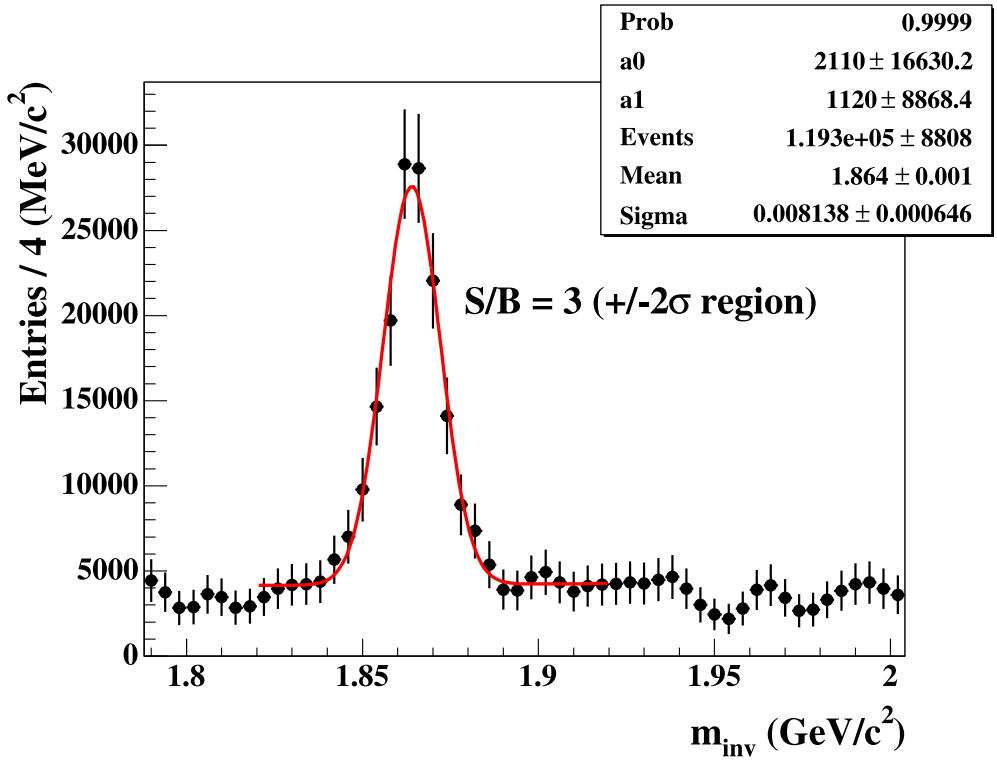

Figure 12: Invariant mass simulated signal plus background spectrum. The D^0 peak is clearly visible. Estimated data taking time is about 4 months at 0.1 MHz interaction rate.

[4] B. Müller and X.N. Wang, Probing parton thermalization time with charm production, Phys. Rev. Lett. **68** (1992) 2437.

[5] P. Braun-Munzinger et al., Heavy Flavour Physics, nucl-ph/0105229.

[6] W. Cassing and E. Bratkovskaya, Transport Theories for Heavy Ion Collisions in the 1 AGeV Regime, Phys. Rep. 308 (1999) 165.

[7] Z. Lin and R. Vogt, The A Dependence of Open Charm and Bottom Production, Nucl. Phys. **B544** (1999) 339.

[8] S. Gorbunov and I. Kisel, An analytic formula for track extrapolation in an inhomogeneous magnetic field, CBM note CBM-SOFT-note-2005-001, FutureDAQ note I3HP-FutureDAQ-note-2005-001, 18 March 2005, (`http://www.gsi.de/onTEAM/dokumente/public/DOC-2005-Mar-212_e.html`).